Accurate Distributed Secondary Control for DC Microgrids Considering Communication Delays: A Surplus Consensus-Based Approach

Yuhua Du, *Member, IEEE*, Xiaonan Lu, *Member, IEEE*, and Wenyuan Tang, *Member, IEEE*

***Abstract*—The state-of-the-art dynamic consensus-based microgrid (MG) secondary controls suffer from the communication delay effect. Specifically, the system could not converge to the desired operating points with time-delayed communications. Such deviations are hard to detect in a decentralized manner and could destabilize the system. This paper proposes an accurate distributed secondary controller for DC MGs based on the surplus consensus algorithm. The proposed controller achieves accurate proportional power sharing and average voltage regulation among distributed generators (DGs) with the presence of variable and bounded communication delays. A surplus consensus-based observer is developed. The developed observer is proved robust against variable and bounded communication delays; it tracks the average of a group of dynamic states with zero steady-state deviations, which cannot be done using the conventional dynamic consensus-based observer. The convergence speed of the developed observer is analyzed and a parameter design procedure is presented. Moreover, the delay-dependent stability analysis of DC MG operation with the proposed secondary controller is derived. The marginal delay that leads the system to instability is calculated. At last, the performance of the proposed secondary controller and the developed stability analysis are validated under various scenarios using MATLAB/Simulink.**

***Index Terms*—Communication delay, consensus algorithms, DC microgrid, distributed control, secondary control, surplus consensus.**

I. Introduction

DECENTRALIZED cooperation techniques for distributed generators (DGs) have been favored in recent years [1]. Each DG could operate as an intelligent agent and form an autonomous microgrid (MG) coordinately. The hierarchical control diagram has been widely adopted in the parallel operation of grid-forming DGs. The secondary-level control is introduced to regulate the system operating points as rated, along with additional objectives (e.g., proportional DG power sharing [2], seamless MG topology variation [3], voltage unbalance mitigation [4], etc.). Consensus-based algorithms have been extensively adopted to achieve distributed secondary control among DGs. Multiple agents (DGs) reach *consensus* when they agree on the value of a particular variable. This common value is called *consensus equilibrium* and the negotiation algorithm is called *consensus algorithm* [5].

However, the convergence of the consensus-based secondary control alone is only a sufficient but not necessary condition for a successful secondary regulation, as the system could converge to the undesired steady-state operating points. For example, for a feeder with various bus voltages, accurate regulations of both local bus voltages and proportional DG power sharing (reactive power for AC MGs and active power for DC MGs) are contradictory and could not be achieved simultaneously [6]. To guarantee accurate DG power sharing while maintaining the system operating voltage within an acceptable range, pinning consensus-based secondary control has been developed [6], where all the DGs take part in power sharing regulation, while only a few 'pinning' DGs regulate their operating voltage as rated. To get rid of the challenges in pinning DG selection and allow all the DGs to participate in the secondary voltage regulation, dynamic consensus-based secondary control has been favored [7], where the average DG operating voltage is observed by each DG using dynamic consensus-based observer and regulated as rated.

One practical challenge that keeps the system with the dynamic consensus-based controller from converging to the desired operating points is the communication delay effect. Analytically speaking, the dynamic consensus-based observer could accurately track the average of a group of time-varying states (e.g., DG operating voltages) when no communication delay is presented [8]. However, information exchange between the neighboring agents cannot be done instantaneously in practice and the communication delay varies with many factors (e.g., real-time network traffic, communication protocol, etc.). It has been proved in the literature that with the presence of communication delays, the dynamic consensus-based observer is guaranteed to converge [9], but will result in non-zero steady-state observation errors [10]. Such observation errors are hard to detect and would result in undesired system operating points. For example, how the non-zero communication delays result in deviated average DG operating voltage regulation has been discussed in [11].

Manuscript received April 28, 2021; revised September 19, 2021 and November 5, 2021; accepted January 4, 2022. Date of publication January 10, 2022; date of current version April 22, 2022. Paper no. TSG-00676-2021. *(Corresponding author: Xiaonan Lu).*

Yuhua Du and Xiaonan Lu are with the College of Engineering, Temple University, Philadelphia, PA 19122 USA (e-mail: yuhua.du@temple.edu; xiaonan.lu@temple.edu).

Wenyuan Tang is with the Department of Electrical and Computer Engineering, North Carolina State University, Raleigh, NC 27695 USA (e-mail: wtang8@ncsu.edu).

Color versions of one or more figures in this article are available at https://doi.org/10.1109/TSG.2022.3141395.

Digital Object Identifier 10.1109/TSG.2022.3141395

Methods that achieve accurate distributed average observation with time-delayed communications have been discussed in the literature. It is proved in [12] that accurate averaging can be achieved with the dynamic consensus if both the internal states (i.e., states measured locally) and the external states (i.e., states acquired through communication) are delayed by the exact same time period. This approach, though has been adopted in many works [13]–[15], has the following limitations: 1) By processing with the delayed internal states, the dynamic consensus is no longer robust against communication delay [16]; 2) To ensure the internal states being delayed in accordance with the external states, additional data storage and buffering are required, which lead to additional investments. A ratio consensus-based observer is proposed in [17] that does not introduce intentional delay and could actively eliminate the observation errors resulted from the communication delay. However, the elimination is done periodically, which is unsecured when facing fast-varying delays. Moreover, the elimination period would be prolonged with greater communication delays, which results in less frequent elimination and degraded performance. A PI-consensus based distributed control for AC MG is proposed in [11]. The proposed controller is effective in achieving accurate frequency/average voltage regulation and proportional active/reactive power sharing with variable communication delay. However, the corresponding delay-dependent stability analysis for system operation has not been derived, and the lacking knowledge of the acceptable delay bound would limit the applicability of such a controller in practice.

In this work, a surplus consensus-based secondary controller is proposed for DC MG operation. The main contributions and notable features of this work are listed.

1) A surplus consensus-based observer is developed with consideration of communication delays. The developed observer is inspired by the surplus consensus algorithm from [18], where only the undelayed algorithm is analyzed. The performance of the delayed surplus consensus algorithm is studied for the first time in this paper. It is proved that with the presence of time-varying and bounded communication delays, the developed surplus consensus-based observer is guaranteed to converge and tracks the average with zero steady-state deviations, which cannot be done by the conventional dynamic consensus-based observer.
2) A surplus consensus-based secondary controller for DC MG operation is proposed. The proposed controller achieves accurate average DG operating voltage regulation and proportional DG power sharing with the presence of time-varying and bounded communication delays. The proposed controller represents an improved performance compared with the state-of-the-art techniques, as it is free from the communication delay effect and does not rely on any knowledge of the variable delays.
3) Delay-dependent stability analysis of the DC MG operation with the proposed surplus consensus-based secondary controller is derived. The small-signal modeling of the whole system is developed and the marginal delay that leads the system to stability transition is calculated. The performance of the proposed controller along with the developed delay-dependent stability analysis is validated under various scenarios using the case study.

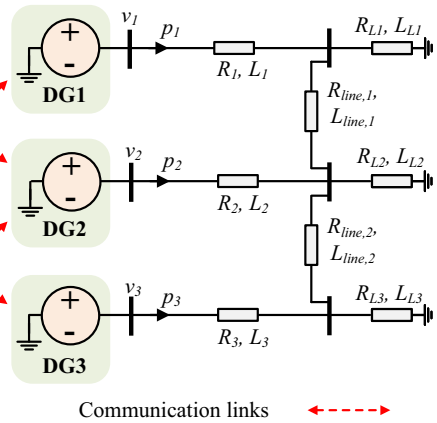

Fig. 1. Autonomous DC MG with parallel operation of grid-forming DGs.

It is noteworthy that although this paper focuses on DC MG secondary control, the developed surplus consensus-based observer could be adopted in a wide range of applications where the accuracy of distributed averaging suffers from the communication delay effect. It is also noteworthy that the aforementioned contributions of the proposed work can not be obtained from the original result in [18]. At last, this paper mainly focuses on the communication delay effect on distributed control, while the other operational challenges in practice (e.g., network packet loss) are not considered. The rest of this paper is constructed as follows. In Section II, the communication delay effect on dynamic consensus-based secondary control for DC MGs is presented. Section III presents a detailed design of the proposed surplus consensus-based secondary control for DC MGs. In Section IV, the delay-dependent stability analysis of DC MG operation with the proposed controller is analyzed and a numerical approach to determine the marginal delay is presented. Section V validates the performance of the proposed controller and the corresponding stability analysis. Finally, the conclusions are drawn in Section VI.

II. Problem Formulation

A sample autonomous DC MG with parallel operation of grid-forming DGs is schematically presented in Fig. 1. Each DG operates as a voltage controlled voltage-source converter (VC-VSC) and adopts the Hierarchical control diagram [19]. In this work, the DGs are coordinated in a decentralized manner using peer-to-peer communication links. The total number of DGs under study is denoted as N. The communication network under study is modeled as an undirected and connected graph, $G = (U, \eta)$, where $U = \{u_1, u_2, \ldots, u_N\}$ denotes the set of agents, and $\eta \subseteq U \times U$ denotes valid communication links among agents. Denote $\mathbf{A} = \{a_{ij}\}$ as the *Adjacency Matrix* where $a_{ij} = 1 = a_{ji}$ if and only if $\{u_i, u_j\} \in \eta$, otherwise $a_{ij} = 0$; denote $\mathbf{D} = \{d_{ii}\}$ as the *Degree Matrix* where $d_{ii} = \sum_{i,j\in U}^{N} a_{ij}$; the corresponding Laplacian matrix, $\mathbf{L}$ is defined as $\mathbf{L} = \mathbf{D} - \mathbf{A}$. The

communication delay from agent i to agent j is denoted as τ_{ij}. It is assumed that $\tau_{ij} \in (0, \tau_u]$ is time-varying and bounded in the subsequent analysis unless otherwise stated, where τ_u represents the upper bound. The probability distribution function (PDF) of τ_{ij} is denoted as $f_{ij}(\varsigma)$, where $\int_0^{\tau_u} f_{ij}(\varsigma)d\delta = 1$ and $x_j(t-\tau_{ij}) = \int_0^{\tau_u} f_{ij}(\varsigma)x_j(t-\varsigma)d\varsigma$ [10]. It is noteworthy that the communication delays under study are different among communication links, and information from various agents that are sent latter could arrive earlier at one common receiving agent. It is also noteworthy that the knowledge of τ_{ij} is not available to agent i in the subsequent analysis, and each agent operates with the latest data it receives from its neighboring agents without knowing the exact time period each data is delayed during transmission. At last, for presentation purpose, denote $\mathbf{I}$ as the identity matrix of proper size, $\mathbf{1}$ and $\mathbf{0}$ as the all ones and all zeros column vector of proper size, respectively.

Conventional voltage controller for the *ith* VC-VSC interfaced DG could be presented as [15]:

$$v_i(t) = V^* - m_i p_i(t) + e_i(t) \tag{1}$$

where $v_i(t)$ and V^* are the operating and rated voltage, respectively; m_i is the P-V droop gain; $p_i(t)$ is the DG output power and $e_i(t)$ is the secondary control variable. With consideration of time-delayed communications, conventional dynamic consensus-based secondary control that achieves proportional DG power sharing and average DG operating voltage regulation is presented:

$$\dot{e}_i(t) = -k_v\big[\overline{v}_i(t) - V^*\big] - k_p \sum_{i,j\in U} a_{ij}\big[m_i p_i(t) - m_j p_j\big(t-\tau_{ij}\big)\big] \tag{2}$$

where k_v and k_p are the designed control gains; $\overline{v}_i(t)$ represents the observed average operating voltage among DGs, i.e., $\overline{v}_i(t) = \frac{1}{N}\sum_{i=1}^N v_i(t)$ by design. The value of $\overline{v}_i(t)$ is available to the local controller on agent i through distributed average observation in a decentralized manner. As the controllers in (2) converges and the system is under steady-state (i.e., $\dot{e}_i(t) = 0$ when $t \to \infty$), it is guaranteed that both terms on the right side of (2) equal to zero, respectively (detailed proof regarding this claim can be found in Appendix A). Accurate power sharing among DGs is achieved, as $m_i p_i(t) = m_j p_j(t-\tau_{ij}) = m_j p_j(t)$. Meanwhile, the observed average operating voltage among DGs is regulated to rated, as $\overline{v}_i(t) = V^*$.

Conventionally, the average DG operating voltage $\overline{v}_i(t)$ is observed by each DG using the standard dynamic consensus algorithm [10]:

$$\overline{v}_i(t) = v_i(t) - \kappa \int_0^t \left\{ \sum_{i,j\in U} a_{ij}\big[\overline{v}_i(r) - \overline{v}_j\big(r-\tau_{ij}\big)\big] \right\} dr \tag{3}$$

where $\kappa > 0$ is a designed control gain. With absence of communication delays (i.e., $\tau_{ij} = 0$ for $i, j \in U$), the average DG operating voltage could be accurately tracked by each agent as the controller converges [8], i.e., $\lim_{t\to\infty}[\overline{v}_i(t) - \frac{1}{N}\sum_{i=1}^N v_i(t)] = 0$.

With consideration of time-delayed communications, it is proved in the literature that the stability of the dynamic consensus algorithm in (3) is independent of the communication delays [9], i.e., algorithm (3) guarantees to converge with $\tau_{ij} \in (0, \tau_u]$ for $i, j \in U$. However, each DG tracks the average DG operating voltage with steady-state errors. Specially, consider introducing a set of step variations to the DG operating voltage, i.e., $v_i(s) = \frac{\Delta v_i}{s}$. If the communication delays are identical, i.e., $\tau_{ij} = \tau_{ji} = \tau$ with $f_{ij}(\varsigma) = f_{ji}(\varsigma) = f(\varsigma)$, the resulted equilibrium variation in (3) is calculated as [10]: $\Delta c_{\overline{v},d} = \frac{1}{N(1+\kappa\overline{\tau})}\sum_{i=1}^N \Delta z_i$, where $\overline{\tau} = \frac{1}{N}(\sum_{i=1}^N d_{ii})\int_0^{\tau_u} \varsigma f(\varsigma)d\varsigma$ is the equivalent mean of delay. Compared to the actual variation under track $\Delta c_{\overline{v},a} = \frac{1}{N}\sum_{i=1}^N \Delta v_i$, the observation error is: $\Delta c_{\overline{v},a} - \Delta c_{\overline{v},d} = \frac{\kappa\overline{\tau}}{N(1+\kappa\overline{\tau})}\sum_{i=1}^N \Delta v_i$ and thus $\lim_{t\to\infty}[\overline{v}_i(t) - \frac{1}{N}\sum_{i=1}^N v_i(t)] \neq 0$. It could also be concluded from (3) that after the controller converges and $\overline{v}_i(t) = \overline{v}_j(t) = c_{\overline{v}}$ remain constant, $v_i(t)$ and thus $\frac{1}{N}\sum_{i=1}^N v_i(t)$ would also remain constant, and the system operates with a constant regulation error, which degrades the performance of voltage secondary regulation in DC MGs.

III. Proposed Surplus Consensus-Based Secondary Controller for VC-VSC in DC MGs

A. Surplus Consensus-Based Observer

To guarantee convergence while achieving accurate average observation, a surplus consensus-based observer with the presence of communication delays is developed:

$$x_i(t) = z_i(t) - \kappa \int_0^t \left\{ \left[\sum_{i,j\in U} a_{ij}\big[x_i(r) - x_j(r-\tau_{ij})\big] - \varepsilon s_i(r) \right\} dr \tag{4a}$$

$$s_i(t) = \kappa \int_0^t \left\{ \sum_{i,j\in U} a_{ij}[x_i(r) - x_j(r-\tau_{ij})] - \varepsilon s_i(r) - \sum_{i,j\in U} a_{ij}[s_i(r) - s_j(r-\tau_{ij})] \right\} dr \tag{4b}$$

where $s_i(t)$ is the surplus state of agent i and $\varepsilon > 0$ is a constant control gain. The initial conditions are set as $x_i(0) = z_i^0$, $s_i(0) = 0$ and $x(t) = s(t) = 0$ for $t \in [-\tau_u, 0)$.

The convergence of the proposed observer is first analyzed. Denote matrix $\mathbf{f}$ as a weighted adjacent matrix where $\mathbf{f}(i,j) = f_{ij}(\varsigma)$ if $a_{ij} = 1$, otherwise $\mathbf{f}(i,j) = 0$. It is noteworthy that compared to the adjacent matrix $\mathbf{A}$, matrix $\mathbf{f}$ is not necessarily symmetric, as $f_{ij} \neq f_{ji}$. By substituting $x_j(t-\tau_{ij}) = \int_0^{\tau_u} f_{ij}(\varsigma)x_j(t-\varsigma)d\varsigma$ and $s_j(t-\tau_{ij}) = \int_0^{\tau_u} f_{ij}(\varsigma)s_j(t-\varsigma)d\varsigma$, the proposed observer in (4) is expressed in vector form as:

$$\dot{\mathbf{x}}(t) = \dot{\mathbf{z}}(t) - \kappa\left[\mathbf{D}\mathbf{x}(t) - \int_0^{\tau_u} \mathbf{f}(\varsigma)\mathbf{x}(t-\varsigma)d\varsigma - \varepsilon\mathbf{s}(t)\right] \tag{5a}$$

$$\dot{\mathbf{s}}(t) = \kappa\left[\mathbf{D}\mathbf{x}(t) - \int_0^{\tau_u} \mathbf{f}(\varsigma)\mathbf{x}(t-\varsigma)d\varsigma - \varepsilon\mathbf{s}(t) - \mathbf{D}\mathbf{s}(t) - \int_0^{\tau_u} \mathbf{f}(\varsigma)\mathbf{s}(t-\varsigma)d\varsigma\right] \tag{5b}$$

where $\mathbf{x}$, $\mathbf{z}$ and $\mathbf{s}$ are the state vectors of x_i, z_i and s_i, respectively. It is noteworthy that in (5), the receiving states x_j and s_j at agent i are delayed by the same time period, τ_{ij} and thus share the same PDF, f_{ij}. This assumption is reasonable, because in practice the sending states from agent j would be delivered to agent i in the same data package, and thus be delayed by the exact same period. Denote $\mathbf{F} = \{F_{ij}(\varphi)\}$ where $F_{ij}(\varphi) = \int_0^{\tau_u} e^{-\varphi\varsigma} f_{ij}(\varsigma)d\varsigma$ is the Laplacian transform of f_{ij}. The characteristic equation of (5) is derived as:

$$det\left(\begin{bmatrix} \lambda\mathbf{I}+\mathbf{D}-\mathbf{F}(\lambda) & -\varepsilon\mathbf{I} \\ -\mathbf{D}+\mathbf{F}(\lambda) & \lambda\mathbf{I}+\varepsilon\mathbf{I}+\mathbf{D}-\mathbf{F}(\lambda) \end{bmatrix}\right) = 0 \quad (6)$$

Detailed derivations from (5) to (6) can be found in Appendix B. It can be proved that (6) has a simple root at zero and the other roots with negative real parts. The following lemma is used for the subsequent analysis.

Lemma 1: Under an undirected and connected network, the characteristic equation $det[\lambda\mathbf{I}+\mathbf{D}-\mathbf{F}(\lambda)] = 0$ has one simple root at zero and the other roots with negative real parts, and the zero root corresponds to the zero eigenvalue of $\mathbf{L} = \mathbf{D} - \mathbf{A}$.

Proof: It is observed that $det[\lambda\mathbf{I} + \mathbf{D} - \mathbf{F}(\lambda)] = 0$ is the characteristic equation of (3), and it has been proved in [9] that this characteristic equation has one simple root at zero and the other roots with negative real part. When $\lambda = 0$, $F_{ij}(0) = \int_0^{\tau_u} f_{ij}(\varsigma)d\varsigma = 1$ and $\mathbf{F}(0) = \mathbf{A}$, thus the simple root at zero corresponds to the zero eigenvalue of $\mathbf{L} = \mathbf{D} - \mathbf{A}$. ■

Referring to Lemma 1, (6) can be simplified using Schur complement as: $det([\lambda\mathbf{I}+\mathbf{D}+\varepsilon\mathbf{I}-\mathbf{F}(\lambda)]-[-\mathbf{D}+\mathbf{F}(\lambda)][\lambda\mathbf{I}+\mathbf{D}-\mathbf{F}(\lambda)]^{-1}[-\varepsilon\mathbf{I}]) = det([\lambda\mathbf{I}+\mathbf{D}-\mathbf{F}(\lambda)][\lambda\mathbf{I}+\mathbf{D}-\mathbf{F}(\lambda)]) = det[\lambda\mathbf{I}+\mathbf{D}-\mathbf{F}(\lambda)]det[\lambda\mathbf{I}+\mathbf{D}-\mathbf{F}(\lambda)] = 0$. It can be concluded that (6) has one simple root at zero that corresponds to the zero eigenvalue of $\mathbf{L}$ and the other roots with negative real part. In other words, it is proved that under undirected and connected network, the proposed observer in (4) is guaranteed to reach consensus regardless of variable communication delay. This convergence conclusion is drawn on f_{ij} in general forms; it is neither achieved by probability nor limited to any specific expressions or values of f_{ij}.

The consensus equilibrium of the proposed observer is then analyzed. Since the observer is guaranteed to reach consensus, i.e., $c_x = x_i(t) = x_j(t)$ and $c_s = s_i(t) = s_j(t)$ when $t \to \infty$, (4b) in steady-state is reduced to:

$$\dot{s}_i(t) = -\varepsilon s_i(t) \quad (7)$$

As the observer converges, $\dot{s}_i(t) = 0$, and it can be easily concluded that $c_s = 0$.

For analysis purposes, it is first assumed that $\mathbf{z} = \mathbf{z}_0$ remains static and thus $\dot{\mathbf{z}} = 0$. The proposed observer in (5) can be further expressed in matrix form as:

$$\begin{bmatrix} \dot{\mathbf{x}}(t) \\ \dot{\mathbf{s}}(t) \end{bmatrix} = \kappa\mathbf{G}\begin{bmatrix} \mathbf{x}(t) \\ \mathbf{s}(t) \end{bmatrix} + \kappa\int_0^{\tau_u} \mathbf{G_f}\begin{bmatrix} \mathbf{x}(t-\delta) \\ \mathbf{s}(t-\delta) \end{bmatrix} d\delta \quad (8)$$

where $\mathbf{G} = \begin{bmatrix} -\mathbf{D} & \varepsilon\mathbf{I} \\ \mathbf{D} & -\mathbf{D}-\varepsilon\mathbf{I} \end{bmatrix}$ and $\mathbf{G_f} = \begin{bmatrix} \mathbf{f} & \mathbf{0} \\ -\mathbf{f} & \mathbf{f} \end{bmatrix}$. It is noteworthy that: $\int_0^{\tau_u} \mathbf{G_f} d\delta = \begin{bmatrix} \mathbf{A} & \mathbf{0} \\ -\mathbf{A} & \mathbf{A} \end{bmatrix} = \mathbf{G_A}$, and $\mathbf{1}^T(\mathbf{G} + \mathbf{G}_A) = \mathbf{0}^T$.

The following relationship can be derived:

$$\begin{aligned} &\frac{\partial}{\partial t}\mathbf{1}^T\left(\begin{bmatrix} \mathbf{x}(t) \\ \mathbf{s}(t) \end{bmatrix} + \kappa\int_0^{\tau_u}\int_{t-\delta}^{t} \mathbf{G_f}\begin{bmatrix} \mathbf{x}(r) \\ \mathbf{s}(r) \end{bmatrix} drd\delta\right) \\ &= \mathbf{1}^T\left(\begin{bmatrix} \dot{\mathbf{x}}(t) \\ \dot{\mathbf{s}}(t) \end{bmatrix} + \kappa\int_0^{\tau_u} \mathbf{G_f}\begin{bmatrix} \mathbf{x}(t)-\mathbf{x}(t-\delta) \\ \mathbf{s}(t)-\mathbf{s}(t-\delta) \end{bmatrix} d\delta\right) \\ &= \kappa\mathbf{1}^T\left(\mathbf{G}\begin{bmatrix} \mathbf{x}(t) \\ \mathbf{s}(t) \end{bmatrix} + \int_0^{\tau_u} \mathbf{G_f}\begin{bmatrix} \mathbf{x}(t-\delta) \\ \mathbf{s}(t-\delta) \end{bmatrix} d\delta + \mathbf{G_A}\begin{bmatrix} \mathbf{x}(t) \\ \mathbf{s}(t) \end{bmatrix}\right. \\ &\qquad \left. - \int_0^{\tau_u} \mathbf{G_f}\begin{bmatrix} \mathbf{x}(t-\delta) \\ \mathbf{s}(t-\delta) \end{bmatrix} d\delta\right) \\ &= \kappa\mathbf{1}^T(\mathbf{G}+\mathbf{G_A})\begin{bmatrix} \mathbf{x}(t) \\ \mathbf{s}(t) \end{bmatrix} = 0 \end{aligned} \quad (9)$$

Thus, it can be concluded from (9) that:

$$\mathbf{1}^T\left(\begin{bmatrix} \mathbf{x}(t) \\ \mathbf{s}(t) \end{bmatrix} + \kappa\int_0^{\tau_u}\int_{t-\delta}^{t} \mathbf{G_f}\begin{bmatrix} \mathbf{x}(r) \\ \mathbf{s}(r) \end{bmatrix} drd\delta\right) \text{ is constant.}$$

As previously discussed, the observer in (8) is guaranteed to converge. Recall the fact that $x_i(t) = s_i(t) = 0$ for $t \in [-\tau_u, 0)$, the following relationships can be derived by setting $t = 0$ and $t \to \infty$, respectively:

$$\begin{aligned} &\mathbf{1}^T\left(\begin{bmatrix} \mathbf{x}(t) \\ \mathbf{s}(t) \end{bmatrix} + \kappa\int_0^{\tau_u}\int_{-\delta}^{0} \mathbf{G_f}\begin{bmatrix} \mathbf{x}(r) \\ \mathbf{s}(r) \end{bmatrix} drd\delta\right) = \mathbf{1}^T\begin{bmatrix} \mathbf{x}_0 \\ \mathbf{s}_0 \end{bmatrix} \\ &= \mathbf{1}^T\left(\begin{bmatrix} c_x\mathbf{1} \\ c_s\mathbf{1} \end{bmatrix} - \kappa\int_0^{\tau_u} \mathbf{G_f}\begin{bmatrix} c_x\mathbf{1} \\ c_s\mathbf{1} \end{bmatrix} d\delta\right) = \mathbf{1}^T(\mathbf{I}-\kappa\mathbf{G_A})\begin{bmatrix} c_x\mathbf{1} \\ c_s\mathbf{1} \end{bmatrix} \\ &= \mathbf{1}^T\begin{bmatrix} \mathbf{I}-\kappa\mathbf{A} & \mathbf{0} \\ \kappa\mathbf{A} & \mathbf{I}-\kappa\mathbf{A} \end{bmatrix}\begin{bmatrix} c_x\mathbf{1} \\ c_s\mathbf{1} \end{bmatrix} \end{aligned} \quad (10)$$

Recall the fact that $c_s = 0$, it is derived from (10) that:

$$\mathbf{1}^T\mathbf{x}_0 + \mathbf{1}^T\mathbf{s}_0 = Nc_x + Nc_s - \kappa c_s\mathbf{1}^T\mathbf{A}\mathbf{1} = Nc_x \quad (11)$$

It is derived from (11) that $c_x = \frac{1}{N}\mathbf{1}^T(\mathbf{x}_0 + \mathbf{s}_0) = \frac{1}{N}\mathbf{1}^T\mathbf{z}_0$. At last, assume the observer is initially under equilibrium c_x' and consider introducing a set of step variations, $\Delta\mathbf{z}$ over $\mathbf{z}$. The new consensus equilibrium, c_x can be calculated as:

$$c_x = \frac{1}{N}\mathbf{1}^T(\Delta\mathbf{z} + \mathbf{z}_0) = \frac{1}{N}\mathbf{1}^T\Delta\mathbf{z} + c_x' \quad (12)$$

Thus, it is proved from (12) that the proposed observer tracks the average variation accurately, as $\Delta c_x = c_x - c_x' = \frac{1}{N}\sum_{i=1}^{N}\Delta z_i(t)$. In conclusion, the proposed observer is robust against communication delays and tracks the average of interest with zero steady-state deviations. The aforementioned results regarding the performance of the developed surplus consensus-based observer in (4) are summarized as follows:

Theorem 1: Under an undirected and connected communication network, the consensus algorithm in (4) is guaranteed to reach consensus with time-varying and bounded communication delays. Furthermore, the average of interest is tracked with zero steady-state error, i.e., for $i = 1, \ldots, N$:

$$\lim_{t\to\infty}[x_i(t) - \frac{1}{N}\sum_{i=1}^{N} z_i(t)] = 0 \text{ and } \lim_{t\to\infty} s_i(t) = 0.$$

At last, a parameter design procedure for ε with a given κ is developed. Denote the transfer function matrix in (4) as $\mathbf{M}$, the convergence speed of the proposed observer is governed by

the second largest eigenvalue of $\mathbf{M}$, where $\lambda_1 = 0 > Re(\lambda_2) \geq \cdots \geq Re(\lambda_{2N})$. Given $\mathbf{M}$ contains time-varying elements (i.e., τ_{ij}), it is concluded that λ_2, and thus the convergence speed of the proposed observer is also time-varying.

To better understand the characteristics of λ_2, the undelayed observer is analyzed where $\tau_{ij} = 0$. In this case, $\mathbf{M} = \mathbf{G} + \mathbf{G_A}$ and the eigenvalues of $\mathbf{M}$ are expressed as [18]:

$$\lambda(\mathbf{M}) = \gamma_i^{\pm} = \kappa \frac{-(2\mu_i + \varepsilon) \pm \sqrt{\varepsilon^2 + 4\mu_i \varepsilon}}{2} \leq 0 \quad (13)$$

where $\mu_i \geq 0$ is the eigenvalue of $\mathbf{L}$.

It is observed from (13) that $\lambda(\mathbf{M})$, and thus the convergence speed of the undelayed observer is positively correlated to the value of κ. With a given κ, $\mu_1 = 0$ corresponds to two eigenvalues of $\mathbf{M}$, where $\gamma_1^+ = 0$ and $\gamma_1^- = -\kappa\varepsilon$. As previously discussed, $\mathbf{M}$ has one eigenvalue at zero and the other eigenvalues being negative, and λ_2 can be expressed as:

$$\lambda_2 = max\left(\gamma_1^-, \gamma_i^+\right) \quad \text{for } i = 2, \ldots, n \quad (14)$$

Referring to (13) and (14), the characteristics of λ_2 with the variations of $\varepsilon > 0$ is analyzed:

1) When ε is sufficiently small (i.e., $\varepsilon \approx 0$), $\lambda_2 = \gamma_1^- = -\kappa\varepsilon$. In this case, $\partial_\varepsilon \lambda_2 = -\kappa < 0$, which indicates that greater value of ε would result in a smaller value of λ_2 and thus greater convergence speed.
2) When $\varepsilon > (2\sqrt{2} - 2)\mu_k$, $\lambda_2 = \gamma_k^+ > \gamma_1^-$ where μ_k corresponds to the γ_k^+ that satisfies $\gamma_k^+ = max(\gamma_i^+)$ for $i = 2, \ldots, n$. In this case, λ_2 is a continuous piece-wise function of ε that is determined by μ_i for $i = 2, \ldots, n$.
3) When ε is sufficiently large (i.e., $\varepsilon \approx \infty$), $\lambda_2 = \gamma_k^+ \approx 0$. In this case, $\partial_\varepsilon \lambda_2 = \kappa(-0.5 + \frac{\varepsilon + 2\mu_k}{2\sqrt{\varepsilon^2 + 4\mu_k\varepsilon}}) = \kappa \frac{\sqrt{\varepsilon^2 + 4\mu_k\varepsilon + 4\mu_k^2} - \sqrt{\varepsilon^2 + 4\mu_k\varepsilon}}{2\sqrt{\varepsilon^2 + 4\mu_k\varepsilon}} > 0$, which indicates that a greater value of ε would result in greater value of λ_2 and thus slower convergence speed.

It is observed that λ_2 is a continuous piece-wise function of $\varepsilon \in (0, \infty)$ for the undelayed observer. Given the fact that $\lambda_2|_{\varepsilon \to 0} = \lambda_2|_{\varepsilon \to \infty} \approx 0$, there must exist an $\varepsilon = \varepsilon_{opt}$ that results in the minimum value of λ_2, referring to the *Extreme Value Theorem*. In conclusion, for a given observer with a designed κ and an explicit network structure, the ε_{opt} that results in the fastest convergence speed for the undelayed observer could be calculated by traversing the values of $\varepsilon > 0$ in (13). Specifically, the value of ε could be iteratively increased from 0 at a designed searching step $\Delta\varepsilon$, and the resulted values of λ_2 at each iteration could be compared to obtain the value of ε_{opt}. The value of ε for the delayed observer is then designed as $\varepsilon = \varepsilon_{opt}$. It is noteworthy that the optimal value of ε is developed based on rigorous analytical derivations and numerically obtained for practical implementation purposes. When the system structure changes, the control gains could be modified by each controller with access to the updated communication network structure, which could be done in a distributed manner [20].

B. Surplus Consensus-Based Secondary Controller

To achieve reliable secondary regulations with time-delayed communications, a surplus consensus-based secondary controller is proposed:

$$\dot{e}_i(t) = k_v V^* - k_p m_i p_i(t) + x_i(t) \quad (15a)$$

$$x_i(t) = -\kappa \int_0^t \left\{ \sum_{i,j \in U} a_{ij}\left[x_i(t) - x_j\left(t - \tau_{ij}\right)\right] - \varepsilon s_i(t) \right\} dt + k_p m_i p_i(t) - k_v v_i(t) \quad (15b)$$

$$s_i(t) = \kappa \int_0^t \left\{ \sum_{i,j \in U} a_{ij}\left[x_i(t) - x_j\left(t - \tau_{ij}\right)\right] - \varepsilon s_i(t) - \sum_{i,j \in U} a_{ij}\left[s_i(t) - s_j\left(t - \tau_{ij}\right)\right] \right\} dt \quad (15c)$$

Based on the previous analysis, as the controllers in (15) converges, $x_i(t) = \frac{1}{N}\sum_{i=1}^{N}\left[k_p m_i p_i(t) - k_v v_i(t)\right]$ regardless of the delay, and (15a) can be expressed as:

$$0 = -k_v \left[\frac{1}{N} \sum_{i=1}^{N} v_i(t) - V^* \right] - k_p \left[m_i p_i(t) - \frac{1}{N} \sum_{i=1}^{N} m_i p_i(t) \right] \quad (16)$$

It is proved that each terms of (16) equals to zero, respectively as the controller converges (detailed proof can be found in Appendix A). Referring to (16), it is observed that when the proposed secondary controller converges, the power output of each DG is accurately regulated to be proportional to its power capacity as $m_i p_i(t) = \frac{1}{N}\sum_{i=1}^{N} m_i p_i(t) = m_j p_j(t)$, and thus $\frac{p_i}{p_j} = (\frac{m_i}{m_j})^{-1} = \frac{P_{i,rate}}{P_{j,rate}}$ where $P_{i,rate}$ is the power capacity of the *ith* DG; the average operating voltage among DGs is regulated to rated, as $\frac{1}{N}\sum_{i=1}^{N} v_i(t) = \bar{v} = V^*$. In case the power output of a certain DG is limited due to abnormal contingencies, such a non-dispatchable DG losses its grid-forming capability and operates as an inverse constant power load, while the system's operating states could still be well-regulated by the remaining grid-forming DGs under the proposed controller.

Compared with the conventional control approach in (2), the proposed controller represents an improved performance since it achieves accurate regulation with the presence of variable communication delays. It is also noteworthy that compared to the approach in (2), the proposed controller (15) requests the same number of variables to be exchanged between the two neighboring agents, which would not result in additional network traffics and thus communication delays. At last, a control diagram of the proposed controller for VC-VSC interfaced DG operation is shown in Fig. 2.

IV. Stability Analysis of DC MG Operation With the Proposed Secondary Controller

Although this work mainly focused on improving the regulation accuracy of consensus-based secondary control with

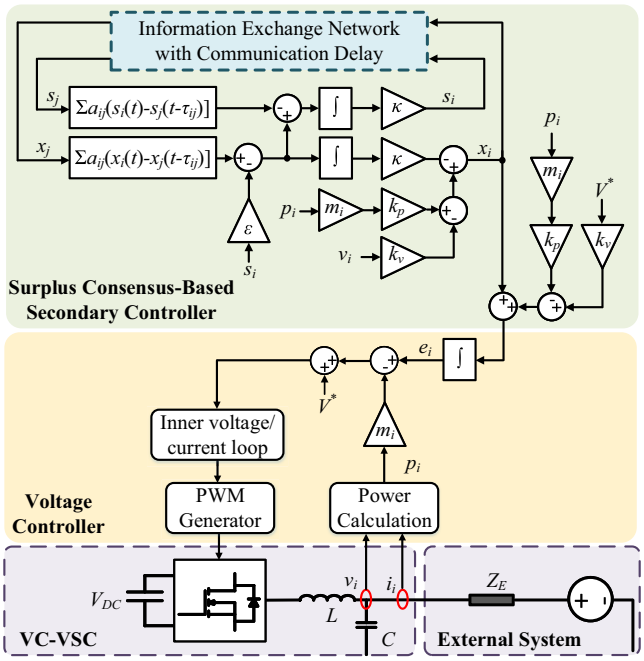

Fig. 2. Control diagram of VC-VSC with the proposed surplus consensus-based secondary controller.

time-delayed communications, delay-dependent stability analysis is also critical for power system operation [21]. As previously discussed, the proposed surplus consensus-based secondary controller achieves accurate regulation as long as the delayed system converges. Thus it is critical to find out the marginal delay that would drive the system to marginal stability. Although the developed surplus consensus-based observer alone is robust against communication delay, the operational stability of the whole system is not guaranteed and should be carefully studied. In this section, the small-signal stability of DC MG operation with the proposed controller is analyzed. In the subsequent analysis, the variable delays are represented by an identical delay, i.e., $\tau_{ij} = \tau$ for simplification [22].

A. Small-Signal Modeling of DC MG

The derived small-signal modeling of DC MG contains two major parts, namely DG modeling and network modeling. The control diagram of the DG under study is presented in Fig. 2, where *P-V* droop control is adopted as the primary control and the proposed surplus consensus-based secondary controller is adopted as the secondary control. For each DG, its instantaneous output power is obtained using a low-pass filter, and the dynamics of p_i is described as:

$$\dot{p}_i = \frac{\omega_c}{s+\omega_c} v_i i_i \tag{17}$$

where ω_c is the cut-off frequency of the low-pass filter and i_i is the DG operating current.

Referring to (1), (15) and (17), the small signal model of the DG under study is derived in matrix form as:

$$\Delta\dot{\mathbf{y}}(t) = \mathbf{W}\Delta\mathbf{y}(t) + \mathbf{W}_d\Delta\mathbf{y}(t-\tau) + \mathbf{W}_I\Delta\mathbf{i}(t) \tag{18}$$

where $\Delta\mathbf{y} = [\Delta p_1, \ldots, \Delta p_n, \Delta v_1, \ldots, \Delta v_n, \Delta e_1, \ldots, \Delta e_n, \Delta x_1, \ldots, \Delta x_n, \Delta s_1, \ldots, \Delta s_n]$ and $\mathbf{\Delta i} = [\Delta i_1, \ldots, \Delta i_n]$ are

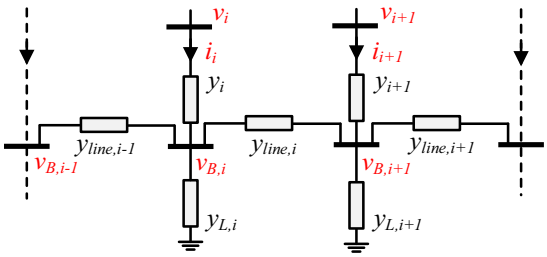

Fig. 3. Equivalent circuit of the DC network under study.

the state vectors. Denote $\hat{\mathbf{i}} = \mathbf{diag}(I_1, \ldots, I_n)$, $\hat{\mathbf{v}} = \mathbf{diag}(V_1, \ldots, V_n)$ and $\hat{\mathbf{m}} = \mathbf{diag}(m_1, \ldots, m_n)$ as three diagonal matrices where I_i and V_i are the system steady-state operating current and voltage at which the small-signal modeling is derived.

The equivalent circuit of the DC network under study is presented in Fig. 3, where y_i represents the line that connects the *ith* DG to the external grid; $y_{line,i}$ is the equivalent admittance of the *ith* transmission line and $y_{L,i}$ represents the *ith* RL load. It is noteworthy Fig. 3 represents a general DC network structure that could be obtained using Kron reduction [23]. Referring to Kirchhoff's Law, it is derived that:

$$y_S v_{B,i}(t) = y_i v_i(t) + y_{line,i-1} v_{B,i-1}(t) + y_{line,i+1} v_{B,i+1}(t). \tag{19}$$

where $y_S = y_i + y_{line,i-1} + y_{line,i+1} + y_{L,i}$ and $v_{B,i}$ is the voltage on the *ith* bus. The small-signal modeling of (19) can be written in matrix form as:

$$\mathbf{\Delta v}_B(t) = (\mathbf{Y}_S)^{-1}\mathbf{Y}\mathbf{\Delta v}(t) \tag{20}$$

where $\mathbf{\Delta v}_B = [\Delta v_{B,1}, \ldots, \Delta v_{B,n}]$ is the state vector, $\mathbf{Y}_S$ is the nodal admittance matrix and $\mathbf{Y} = \mathbf{diag}(y_i)$.

Additionally, the relationship between the bus voltage and DG operating voltage can be expressed as:

$$\mathbf{Y}[\mathbf{\Delta v}(t) - \mathbf{\Delta v}_B(t)] = \mathbf{\Delta i}(t) \tag{21}$$

Following relationship between the DG operating voltage and current can be derived by combining (20) and (21):

$$\mathbf{Y}_N\mathbf{\Delta v}(t) = \mathbf{\Delta i}(t) \tag{22}$$

where $\mathbf{Y}_N = \mathbf{Y}[\mathbf{I} - (\mathbf{Y}_S)^{-1}\mathbf{Y}]$. Substituting (22) into (18), the complete small-signal modeling of the DC MG under study can be expressed as:

$$\Delta\dot{\mathbf{y}}(t) = \mathbf{W}'\Delta\mathbf{y}(t) + \mathbf{W}_d\Delta\mathbf{y}(t-\tau) \tag{23}$$

where $\mathbf{W}' = \mathbf{W} + \mathbf{W}_I\mathbf{Y}_N\begin{bmatrix}\mathbf{0} & \mathbf{I} & \mathbf{0} & \mathbf{0} & \mathbf{0}\end{bmatrix}$.

B. Determination of Marginal Delay

Consider a system that is stable at $\tau = 0$. As the value of τ increases, the marginal delay τ^* is defined as the minimal delay that leads the system to instabilities. The characteristic equation of (23) is derived as:

$$det\left(s\mathbf{I} - \mathbf{W}' - \mathbf{W}_d e^{-\tau s}\right) = 0. \tag{24}$$

Based on the stability theory, the time-delayed linear system in (23) is asymptotically stable if all the roots of (24) lie in the left half of the complex plane. Finding all the roots of (24) is mathematically difficult, as it is a transcendental and implicit

function of s and τ. However, it is possible to locate the critical delays, τ_c, that result in system stability transition, i.e., imaginary roots of (24) where $\lambda_c = \pm j\omega_c$. After finding all the possible critical delays, the next step is to determine in which direction their resulting imaginary eigenvalue crosses the axis. This can be determined using root tendency (RT) [22]:

$$RT|_{s=j\omega_c} = sgn\left[\mathrm{Re}\left(\frac{\partial s}{\partial \tau}|_{s=j\omega_c}\right)\right] \tag{25}$$

As discussed, only the imaginary eigenvalues that result in the system transit from stable to unstable are of interest, which requires $RT|_{j\omega_c} = +1$. At last, if the aforementioned analysis yields to multiple delays, i.e., $\tau_{c,1}, \ldots, \tau_{c,m}$, then the marginal delay is chosen as $\tau^* = \min(\tau_{c,1}, \ldots, \tau_{c,m})$.

To compute the marginal delay for a given system based on the aforementioned analysis, a direct method was proposed in [24]. For the characteristic equations in the following form:

$$A(s) + C(s)e^{-s\tau} = 0 \tag{26}$$

Calculation of ω_c equals to solving the following equation:

$$W\left(\omega^2\right) = A(j\omega)A(-j\omega) - C(j\omega)C(-j\omega) = 0 \tag{27}$$

Equation (27) is a polynomial of ω^2 with no transcendental term and can be solved using standard methods. If there is no positive solution of ω^2 in (27), then there will not be any stability transition. For a positive real root $\omega_{c,i}$, the corresponding critical delay, $\tau_{c,i}$, can be obtained by:

$$\tau_{c,i} = \frac{1}{\omega_{c,i}}\tan^{-1}\left(\frac{\mathrm{Im}\left\{\frac{A(j\omega_{c,i})}{C(j\omega_{c,i})}\right\}}{\mathrm{Re}\left\{-\frac{A(j\omega_{c,i})}{C(j\omega_{c,i})}\right\}}\right) + \frac{2r\pi}{\omega_{c,i}};\ r = 0, 1, \ldots, \tag{28}$$

And the corresponding RT of $\omega_{c,i}$ can be calculated as:

$$RT|_{s=j\omega_{c,i}} = sgn\left[\partial_{\omega^2} W\left(\omega_{c,i}^2\right)\right] \tag{29}$$

The aforementioned direct method provides an exact solution to compute the existing marginal delay. However, formulating $W(\omega^2)$ in (27) is usually non-trivial for a high-order system. A numerical approach to compute the marginal delay is proposed in [25] that does not rely on the exact derivation of $W(\omega^2)$. Define $\xi = \omega_c\tau_c$ and substitute into (24), it can be easily concluded that $e^{j\xi}$ and thus the imaginary roots of (24) vary with ξ at a 2π period. Then by traversing the value of ξ under the range $[0, 2\pi]$, all the $\xi_{c,i}$ that result in imaginary eigenvalues of $\mathbf{W}' + \mathbf{W}_d e^{-j\xi}$, $\pm j\omega_{c,i}$, can be computed. The traversing and the corresponding eigenvalue computation can be easily coded and executed numerically.

Similar to the direct method, if there exists no such $\xi_{c,i}$, then there is no stability transition for the given system. The corresponding critical delay of $\xi_{c,i}$ is computed as:

$$\tau_{c,i} = \frac{\xi_{c,i}}{|\omega_{c,i}|} \tag{30}$$

At last, since the system is stable at $\tau = 0$, the minimal critical delay is guaranteed to result in the system stability transition from stable to unstable. In other words, for $\tau_{c,min} = \min(\tau_{c,1}, \ldots, \tau_{c,m})$ and its corresponding $j\omega_{c,min}$, it is guaranteed that $RT|_{s=j\omega_{c,min}} = +1$ and thus $\tau^* = \tau_{c,min}$.

TABLE I
SYSTEM PARAMETER SETTINGS

Parameters	Values
P-V droop gain	$m = 5.4 \times 10^{-3}$ V/W
Rated DC voltage	$V^* = 380$ V
Power filter cut-off frequency	$\omega_0 = 2\pi$ rad/s
Transmission lines	$R_1 = 0.06\ \Omega$, $L_1 = 0.7$ mH $R_2 = 0.06\ \Omega$, $L_2 = 0.7$ mH $R_3 = 0.06\ \Omega$, $L_3 = 0.7$ mH $R_{line,1} = 0.35\ \Omega$, $L_{line,1} = 1.5$ mH $R_{line,2} = 0.35\ \Omega$, $L_{line,2} = 1.5$ mH
Resistive loads	$R_{L1} = 15.625\ \Omega$, $L_{L1} = 0$ mH $R_{L2} = 156.25\ \Omega$, $L_{L2} = 0$ mH $R_{L3} = 62.5\ \Omega$, $L_{L3} = 0$ mH
Secondary control gains	$\varepsilon = 0.5$, $\kappa = 1$, $k_v = 1$, $k_p = 2$

V. CASE STUDY

The performance of the proposed surplus consensus-based secondary controller is validated with the presence of communication delays on the test feeder shown in Fig. 1, where the communication links among DGs are presented using dashed lines. Three VC-VSC interfaced DGs with identical power capacity are considered and each DG is implemented with droop control along with the secondary controller. The DGs initially operate with only droop control and the proposed secondary control is later initiated at t_1. Detailed system parameter settings can be found in Table I. In this study, the value of ε is designed based on the developed procedure with $\kappa = 1$. The variation of λ_2 with different values of ε is calculated and presented in Fig. 4, where the searching

$$\mathbf{W} = \begin{bmatrix} -\omega_c\mathbf{I} & \omega_c\hat{\mathbf{i}} & \mathbf{0} & \mathbf{0} & \mathbf{0} \\ (\omega_c - k_p)\hat{\mathbf{n}} & -\omega_c\hat{\mathbf{n}}\hat{\mathbf{i}} & \mathbf{0} & \mathbf{I} & \mathbf{0} \\ -k_p\hat{\mathbf{n}} & \mathbf{0} & \mathbf{0} & \mathbf{I} & \mathbf{0} \\ [k_pk_v - \omega_c(k_p + k_v)]\hat{\mathbf{n}} & \omega_c(k_p + k_v)\hat{\mathbf{n}}\hat{\mathbf{i}} & \mathbf{0} & -k_v\mathbf{I} - \kappa\mathbf{D} & \kappa\varepsilon\mathbf{I} \\ \mathbf{0} & \mathbf{0} & \mathbf{0} & \kappa\mathbf{D} & -\kappa(\mathbf{D} - \varepsilon\mathbf{I}) \end{bmatrix}, \mathbf{W}_d = \begin{bmatrix} \mathbf{0} & \mathbf{0} & \mathbf{0} & \mathbf{0} & \mathbf{0} \\ \mathbf{0} & \mathbf{0} & \mathbf{0} & \mathbf{0} & \mathbf{0} \\ \mathbf{0} & \mathbf{0} & \mathbf{0} & \mathbf{0} & \mathbf{0} \\ \mathbf{0} & \mathbf{0} & \mathbf{0} & \kappa\mathbf{A} & \mathbf{0} \\ \mathbf{0} & \mathbf{0} & \mathbf{0} & -\kappa\mathbf{A} & \kappa\mathbf{A} \end{bmatrix}$$

$$\mathbf{W}_I = \begin{bmatrix} \omega_c\hat{\mathbf{v}} \\ -\omega_c\hat{\mathbf{n}}\hat{\mathbf{v}} \\ \mathbf{0} \\ \omega_c(k_p + k_v)\hat{\mathbf{n}}\hat{\mathbf{v}} \\ \mathbf{0} \end{bmatrix}$$

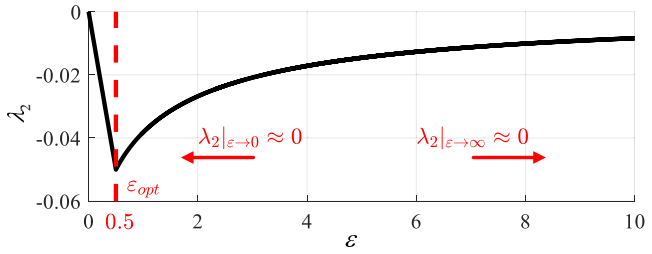

Fig. 4. Variation of λ_2 with different values of ε for the undelayed surplus consensus-based observer.

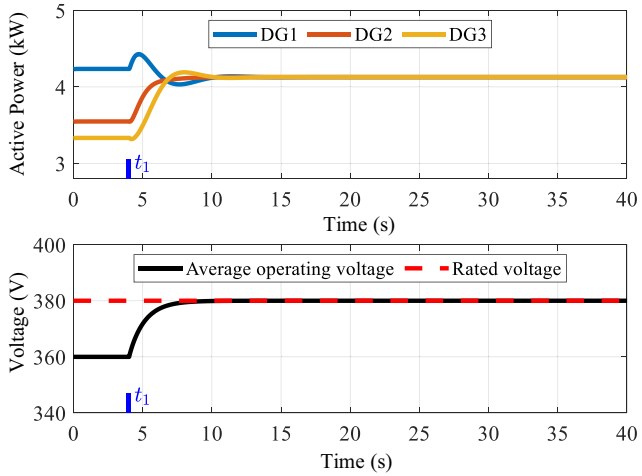

Fig. 5. DG operating states under the proposed surplus consensus-based secondary controller with no communication delay.

step is designed as $\Delta\varepsilon = 0.001$. The value of ε that results in the minimum λ_2 is found to be $\varepsilon = \varepsilon_{opt} = 0.5$. For the given parameter settings, the resulted system marginal delay is calculated as $\tau^* = 1240$ ms.

A. Performance of the Proposed Secondary Controller

The performance of the proposed secondary controller is first validated when no communication delay is presented, i.e., $\tau_{ij} = 0$. The variation of DG power outputs and the average DG operating voltage are shown in Fig. 5, respectively. It is observed that after the proposed controller is initiated, proportional power sharing among DGs is achieved and the average DG operating voltage is regulated as rated. Additionally, to demonstrate the effect of the control gain on convergence speed and validate the proposed parameter design procedure, the variations of DG1 power output under $\varepsilon = \varepsilon_{opt} = 0.5$ and $\varepsilon = 10$ are compared and shown in Fig. 6. It is observed that the undelayed observer converges faster when $\varepsilon = \varepsilon_{opt} = 0.5$, which agrees with the analysis results shown in Fig. 4.

The performance of the proposed controller is then validated under time-varying and bounded communication delay, i.e., $\tau_{ij} \in (0, \tau_u]$. The communication delays on each communication link are designed as $\tau_{12} = 50 + 10sin(6t)$ ms, $\tau_{21} = 75 + 20sin(10t)$ ms, $\tau_{23} = 10 + 5sin(12t)$ ms and $\tau_{32} = 100 + 20sin(15t)$ ms. The various delays are designed to be time-varying and bounded by the calculated marginal delay; they are randomly selected to provide a proof of concept. The

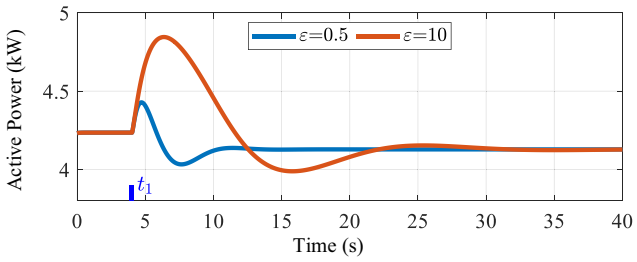

Fig. 6. DG1 power outputs under the proposed surplus consensus-based secondary controller with different ε and no communication delay.

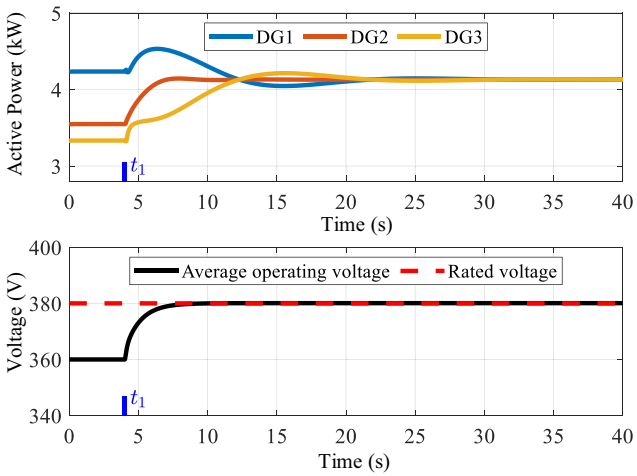

Fig. 7. DG operating states under the proposed surplus consensus-based secondary controller with variable communication delays.

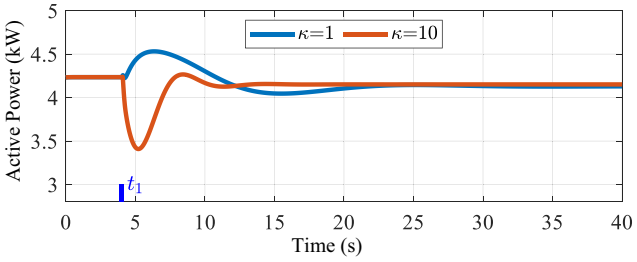

Fig. 8. DG1 power outputs under the proposed surplus consensus-based secondary controller with different κ and the same cyber network conditions.

operating states of each DG under the proposed controller are shown in Fig. 7. It is observed that the proposed controller guarantees accurate regulation with varying communication delays. Both the power sharing and average voltage regulation have been achieved with no steady-state deviations. It can also be observed that compared to that in Fig. 5, the system's settling time in Fig. 7 is extended, which is caused by the introduction of communication delays. Under the same cyber network conditions (i.e., the same communication network topology and the same communication delays), the settling time could be reduced by adopting a greater value of κ. The variations of DG1 power output under $\kappa = 1$ and $\kappa = 10$ are compared and shown in Fig. 8. It can be observed from Fig. 8 that under the same cyber network conditions, the system with a greater value of κ has less settling time but greater overshoot

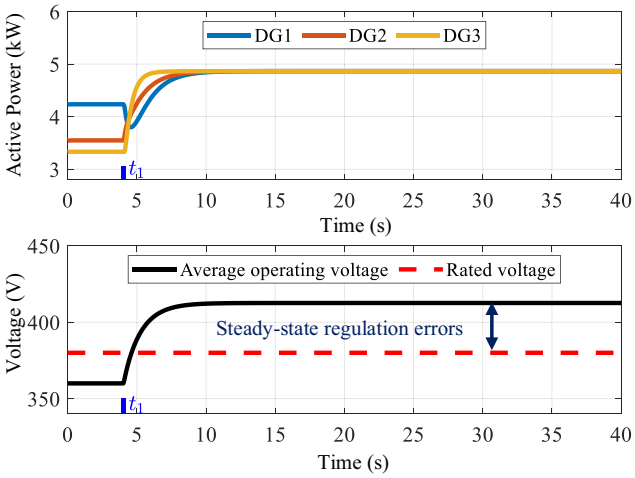

Fig. 9. DG operating states under the conventional dynamic consensus-based secondary controller with variable communication delay.

during the regulation. Such a trade-off indicates that the value of κ can not be arbitrarily large.

B. Comparison With the Conventional Approach

For comparison, the conventional dynamic consensus-based secondary controller shown in (2) is implemented on each DG; it is activated at t_1 and the resulting DG operating states are shown in Fig. 9. It is observed that under time-delayed communications, the system with the conventional dynamic consensus-based secondary controller is able to converge; however, there exist significant steady-state regulation errors over the average voltage regulation. The regulation error is constant, which agrees with the previous discussions. Such errors are caused by the time-delayed communications; they have not only made the system operating voltage exceed the rated value but also overloaded the DGs with extra power outputs, compared to that shown in Fig. 7.

Specifically, as shown in Fig. 9, the average DG operating voltage is under the rated value with only droop control and should be increased by the secondary control, i.e., $\frac{1}{N}\sum_{i=1}^{N}\Delta v_i > 0$. As discussed, the average DG operating voltage observed by the dynamic consensus-based observer would be deviated from its actual value due to the communication delay effect and the observation error is derived as: $\Delta\bar{v}_{i,a} - \Delta\bar{v}_{i,d} = \frac{\kappa\bar{\tau}}{N(1+\kappa\bar{\tau})}\sum_{i=1}^{N}\Delta v_i$, where $\Delta\bar{v}_{i,a}$ and $\Delta\bar{v}_{i,d}$ are the actual and observed average DG operating voltage variations, respectively. This relationship indicates that when $\frac{1}{N}\sum_{i=1}^{N}\Delta v_i > 0$, the observed average DG operating voltage for secondary regulation is less than the actual value. And by regulating the observed voltage as rated, the actual voltage would be greater than the rated value. Because in the DC MG, the power consumption from the impedance-based loads is positively correlated to the system operating voltage, the greater system operating voltage under the conventional dynamic consensus-based secondary controller would request more power outputs from the grid-forming DGs. The results agree with the discussions presented in the previous sections and further validate the effectiveness of the proposed work.

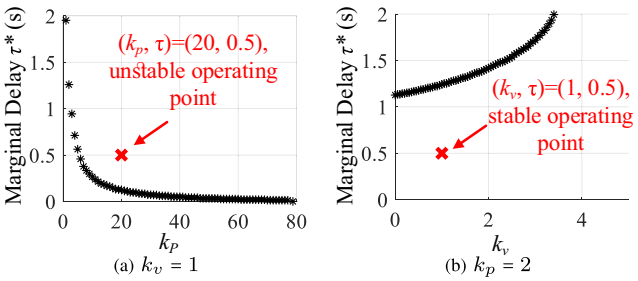

Fig. 10. Marginal delay variations with different values of (a) k_p and (b) k_v.

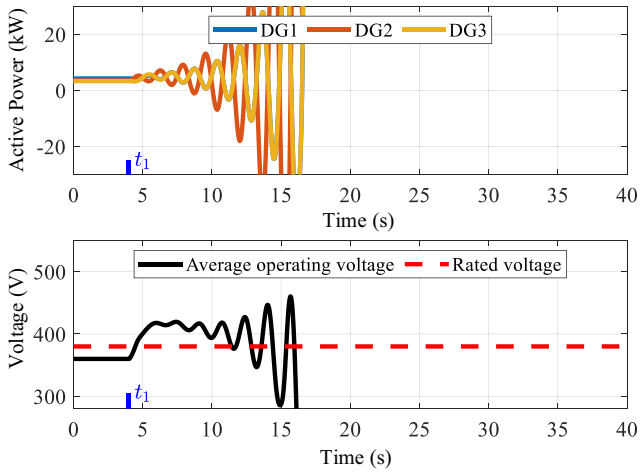

Fig. 11. DG operating states under the proposed surplus consensus-based secondary controller with $k_v = 1$, $k_p = 20$ and $\tau = 500$ ms.

C. System Operational Stability Analysis

At last, how the system's operational stability would be affected by the different selections of secondary control gains is quantitatively analyzed. As previously discussed, it is numerically difficult to calculate all the eigenvalues of the time-delayed system. In this study, the marginal delays under different values of k_p and k_v are calculated, respectively, using the numerical approach presented in Section IV-B and shown in Fig. 10. It is observed from Fig. 10(a) that a greater value of k_p potentially destabilize the system, as it results in a smaller value of τ^*; while the value of τ^* increases with a greater value of k_v and the system is more robust against communication delay, as shown in Fig. 10(b).

To further validate the derived marginal delays, the variations of DG operating points with different selections of k_p and k_v are presented in Figs. 11 and 12. The corresponding operating points are marked in Fig. 10 by red crosses, respectively. It is observed from Fig. 11 that when $k_v = 1$, $k_p = 20$ and $\tau = 500$ ms, the system would lose synchronism when the proposed controller is initiated, which agrees with the results in Fig. 10(a) as $\tau > \tau^*$ in this case. Meanwhile, as shown in Fig. 12, the system is stable when $k_v = 1$, $k_p = 2$ and $\tau = 500$ ms and accurate secondary regulations are achieved, which agrees with the results in Fig. 10(b) as $\tau < \tau^*$ in this case. At last, depending on how the optimization problems are formulated, the optimal values of k_v and k_p could be derived based on the marginal delay τ^*, which are out of the scope in this work.

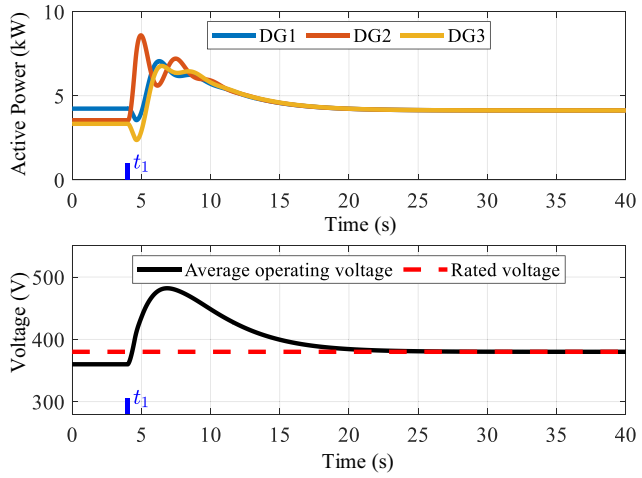

Fig. 12. DG operating states under the proposed surplus consensus-based secondary controller with $k_v = 1$, $k_p = 2$ and $\tau = 500$ ms.

VI. Conclusion

A surplus consensus-based observer is developed. The developed observer tracks the average of interest with variable communication delay. The convergence speed of the proposed observer is analyzed, and a parameter design procedure is developed. A surplus consensus-based secondary controller is proposed for DC MG operation. The proposed secondary controller achieves proportional DG power sharing and average DG voltage regulation with the presence of time-varying and bounded communication delays, which cannot be done using the existing dynamic consensus-based controllers in the literature. The delay-dependent stability of the DC MG operation with the proposed secondary controller is analyzed. The proposed works are validated on a test feeder that operates autonomously in the context of a DC MG. It is concluded from the simulation results that the proposed secondary controller achieves accurate secondary regulations regardless of the communication delay. The derived marginal delays under different selections of secondary control gains are also validated.

Appendix A

As the controller in (2) converges, the following relationship can be observed:

$$0 = k_v\left(\overline{v}_{i,SS} - V^*\right) + k_p \sum_{i,j\in U} a_{ij}\left(m_i p_{i,SS} - m_j p_{j,SS}\right) \quad (31)$$

where $\overline{v}_{i,SS} = \overline{v}_i(\infty)$, $p_{i,SS} = p_i(\infty)$ and $p_{j,SS} = p_j(\infty)$ represent the steady-state value of $\overline{v}_i(t)$, $p_i(t)$ and $p_j(t)$, respectively. For presentation purpose, denote $\Delta\overline{V}_{i,SS} = k_v(\overline{v}_{i,SS} - V^*)$ and $\Delta P_{i,SS} = k_p \sum_{i,j\in U} a_{ij}(m_i p_{i,SS} - m_j p_{j,SS})$, and thus $\Delta\overline{V}_{i,SS} + \Delta P_{i,SS} = 0$ referring to (31).

Given the fact that $\overline{v}_{i,SS} = \overline{v}_{j,SS}$ by design, it can be first observed that $\Delta\overline{V}_{i,SS} = \Delta\overline{V}_{j,SS}$ and thus $\Delta P_{i,SS} = \Delta P_{j,SS}$ on each DG. The communication network under study is undirected and connected, and the term $\Delta P_{i,SS}$ on each DG can be expressed into the matrix form as:

$$\mathbf{\Delta P_{SS}} = k_p \mathbf{L P_{SS}},$$

where $\mathbf{\Delta P_{SS}}$ is a vector that contains the term $\Delta P_{i,SS}$ on each DG, $\mathbf{L}$ is the Laplacian matrix of the communication network among DGs and $\mathbf{P_{SS}}$ is a vector that contains the term $P_{i,SS}$ on each DG. Recall that $\Delta P_{i,SS} = \Delta P_{j,SS}$ as previously proved, the vector $\mathbf{\Delta P_{SS}}$ contains identical elements and can be expressed as:

$$\mathbf{\Delta P_{SS}} = \alpha[\mathbf{1}]_{N\times 1},$$

where α is a constant and $[\mathbf{1}]_{N\times 1}$ represents an N-by-1 all ones vector. Recall the fact that $[\mathbf{1}]_{N\times 1}^T$ is the left eigenvector of $\mathbf{L}$ that corresponds to the eigenvalue $\lambda_1 = 0$ [26], it is derived that:

$$\alpha = \frac{1}{N}[\mathbf{1}]_{N\times 1}^T \alpha[\mathbf{1}]_{N\times 1} = \frac{k_p}{N}[\mathbf{1}]_{N\times 1}^T \lambda_1 \mathbf{P_{SS}} = 0.$$

It is observed that $\alpha = 0$ and thus $\mathbf{\Delta P_{SS}}$ is an all-zeros vector. It can be concluded that $\Delta P_{i,SS} = \Delta P_{j,SS}$ if and only if $\Delta P_{i,SS} = \Delta P_{j,SS} = 0$. Substitute $\Delta P_{i,SS} = 0$ into (31) and it can be derived that $\Delta\overline{V}_{i,SS} = 0$. This completes the proof that both terms on the right side of (3) in the revised manuscript equals to zero, respectively as the controller converges.

As the controller in (16) converges, the following relationship can be observed:

$$0 = k_v\left(\frac{1}{N}\sum_{i=1}^{N} v_{i,SS} - V^*\right) + k_p\left(m_i p_{i,SS} - \frac{1}{N}\sum_{i=1}^{N} m_i p_{i,SS}\right) \quad (32)$$

where $v_{i,SS} = v_i(\infty)$ represents the steady-state value of $v_i(t)$. For presentation purposes, denote $\Delta\overline{V}'_{i,SS} = k_v(\frac{1}{N}\sum_{i=1}^{N} v_{i,SS} - V^*)$ and $\Delta P'_{i,SS} = k_p(m_i p_{i,SS} - \frac{1}{N}\sum_{i=1}^{N} m_i p_{i,SS})$, and thus $\Delta\overline{V}'_{i,SS} + \Delta P'_{i,SS} = 0$ referring to (32).

It can be easily observed that $v_{i,SS} = v_{j,SS}$ as the value of $\frac{1}{N}\sum_{i=1}^{N} v_{i,SS}$ is identical on each DG. Referring to (32), it can be concluded that $\Delta P'_{i,SS} = \Delta P'_{j,SS}$, and thus $m_i p_{i,SS} = m_j p_{j,SS}$ as the value of $\frac{1}{N}\sum_{i=1}^{N} m_i p_{i,SS}$ is identical on each DG. Then it can be further concluded that $m_i p_{i,SS} = m_j p_{j,SS} = \frac{1}{N}\sum_{i=1}^{N} m_i p_{i,SS}$, and thus $\Delta P'_{i,SS} = k_p(m_i p_{i,SS} - \frac{1}{N}\sum_{i=1}^{N} m_i p_{i,SS}) = 0$ and $\Delta\overline{V}'_{i,SS} = -\Delta P'_{i,SS} = 0$. This completes the proof that both terms on the right side of (16) in the revised manuscript equals to zero, respectively as the controller converges.

Appendix B

Equation (5) is first expressed in the Laplace domain:

$$\varphi\mathbf{x}(\varphi) = \varphi\mathbf{z}(\varphi) - \kappa[\mathbf{D}\mathbf{x}(\varphi) - \mathbf{F}(\varphi)\mathbf{x}(\varphi) - \varepsilon\mathbf{s}(\varphi)] \quad (33a)$$

$$\varphi\mathbf{s}(\varphi) = \kappa[\mathbf{D}\mathbf{x}(\varphi) - \mathbf{F}(\varphi)\mathbf{x}(\varphi) - \varepsilon\mathbf{s}(\varphi) - \mathbf{D}\mathbf{s}(\varphi) - \mathbf{F}(\varphi)\mathbf{s}(\varphi)] \quad (33b)$$

where the state vector is $[\mathbf{x}(\varphi), \mathbf{s}(\varphi)]^T$ and the system matrix $\mathbf{A}_{ss}$ can be observed as:

$$\mathbf{A}_{ss} = \kappa\begin{bmatrix} -\mathbf{D} + \mathbf{F}(\varphi) & \varepsilon\mathbf{I} \\ \mathbf{D} - \mathbf{F}(\varphi) & -\varepsilon\mathbf{I} - \mathbf{D} + \mathbf{F}(\varphi) \end{bmatrix}.$$

The resulted characteristic equation can be derived as:

$$det(\lambda\mathbf{I}-\mathbf{A}_{ss}) = det\left(\begin{bmatrix}\lambda\mathbf{I}+\mathbf{D}-\mathbf{F}(\lambda) & -\varepsilon\mathbf{I} \\ -\mathbf{D}+\mathbf{F}(\lambda) & \lambda\mathbf{I}+\varepsilon\mathbf{I}+\mathbf{D}-\mathbf{F}(\lambda)\end{bmatrix}\right)=0.$$

Notice that the positive constant κ is omitted. This completes the derivation of (6).

REFERENCES

[1] T. Morstyn, B. Hredzak, and V. G. Agelidis, "Control strategies for microgrids with distributed energy storage systems: An overview," *IEEE Trans. Smart Grid*, vol. 9, no. 4, pp. 3652–3666, Jul. 2018.

[2] X. Wu *et al.*, "A two-layer distributed cooperative control method for islanded networked microgrid systems," *IEEE Trans. Smart Grid*, vol. 11, no. 2, pp. 942–957, Mar. 2020.

[3] Y. Du, X. Lu, J. Wang, and S. Lukic, "Distributed secondary control strategy for microgrid operation with dynamic boundaries," *IEEE Trans. Smart Grid*, vol. 10, no. 5, pp. 5269–5282, Sep. 2019.

[4] M. Savaghebi, A. Jalilian, J. C. Vasquez, and J. M. Guerrero, "Secondary control scheme for voltage unbalance compensation in an islanded droop-controlled microgrid," *IEEE Trans. Smart Grid*, vol. 3, no. 2, pp. 797–807, Jun. 2012.

[5] W. Ren and R. W. Beard, *Distributed Consensus in Multi-Vehicle Cooperative Control*. London, U.K.: Springer, 2008.

[6] J. W. Simpson-Porco, Q. Shafiee, F. Dörfler, J. C. Vasquez, J. M. Guerrero, and F. Bullo, "Secondary frequency and voltage control of islanded microgrids via distributed averaging," *IEEE Trans. Ind. Electron.*, vol. 62, no. 11, pp. 7025–7038, Nov. 2015.

[7] J. Zhou, S. Kim, H. Zhang, Q. Sun, and R. Han, "Consensus-based distributed control for accurate reactive, harmonic, and imbalance power sharing in microgrids," *IEEE Trans. Smart Grid*, vol. 9, no. 4, pp. 2453–2467, Jul. 2018.

[8] D. P. Spanos, R. Olfati-Saber, and R. M. Murray, "Dynamic consensus on mobile networks," in *Proc. IFAC World Congr.*, 2005, pp. 1–6.

[9] Y. Tian and C. Liu, "Consensus of multi-agent systems with diverse input and communication delays," *IEEE Trans. Autom. Control*, vol. 53, no. 9, pp. 2122–2128, 2008.

[10] F. M. Atay, "Consensus in networks under transmission delays and the normalized Laplacian," *IFAC Proc. Vol.*, vol. 43, no. 2, pp. 277–282, 2010.

[11] M. Shi, X. Chen, J. Zhou, Y. Chen, J. Wen, and H. He, "PI-consensus based distributed control of AC microgrids," *IEEE Trans. Power Syst.*, vol. 35, no. 3, pp. 2268–2278, May 2020.

[12] R. Olfati-Saber and R. M. Murray, "Consensus problems in networks of agents with switching topology and time-delays," *IEEE Trans. Autom. Control*, vol. 49, no. 9, pp. 1520–1533, Sep. 2004.

[13] G. Lou, W. Gu, X. Lu, Y. Xu, and H. Hong, "Distributed secondary voltage control in islanded microgrids with consideration of communication network and time delays," *IEEE Trans. Smart Grid*, vol. 11, no. 5, pp. 3702–3715, Sep. 2020.

[14] H. Zhang, S. Kim, Q. Sun, and J. Zhou, "Distributed adaptive virtual impedance control for accurate reactive power sharing based on consensus control in microgrids," *IEEE Trans. Smart Grid*, vol. 8, no. 4, pp. 1749–1761, Jul. 2017.

[15] V. Nasirian, S. Moayedi, A. Davoudi, and F. L. Lewis, "Distributed cooperative control of DC microgrids," *IEEE Trans. Power Electron.*, vol. 30, no. 4, pp. 2288–2303, Apr. 2015.

[16] J. Lai, H. Zhou, X. Lu, X. Yu, and W. Hu, "Droop-based distributed cooperative control for microgrids with time-varying delays," *IEEE Trans. Smart Grid*, vol. 7, no. 4, pp. 1775–1789, Jul. 2016.

[17] Y. Du, H. Tu, H. Yu, and S. Lukic, "Accurate consensus-based distributed averaging with variable time delay in support of distributed secondary control algorithms," *IEEE Trans. Smart Grid*, vol. 11, no. 4, pp. 2918–2928, Jul. 2020.

[18] S. Kawamura, K. Cai, M. Ye, and Z. Lin, "Tight bound on parameter of surplus-based averaging algorithm over balanced digraphs," *Int. J. Control*, vol. 93, no. 8, pp. 1859–1866, 2020.

[19] J. M. Guerrero, J. C. Vasquez, J. Matas, L. G. de Vicuna, and M. Castilla, "Hierarchical control of droop-controlled AC and DC microgrids—A general approach toward standardization," *IEEE Trans. Ind. Electron.*, vol. 58, no. 1, pp. 158–172, Jan. 2011.

[20] A. Y. Kibangou and C. Commault, "Decentralized Laplacian eigenvalues estimation and collaborative network topology identification," *IFAC Proc. Vol.*, vol. 45, no. 26, pp. 7–12, 2012.

[21] M. Dong, L. Li, Y. Nie, D. Song, and J. Yang, "Stability analysis of a novel distributed secondary control considering communication delay in DC microgrids," *IEEE Trans. Smart Grid*, vol. 10, no. 6, pp. 6690–6700, Nov. 2019.

[22] S. Sönmez, S. Ayasun, and C. O. Nwankpa, "An exact method for computing delay margin for stability of load frequency control systems with constant communication delays," *IEEE Trans. Power Syst.*, vol. 31, no. 1, pp. 370–377, Jan. 2016.

[23] F. Dorfler and F. Bullo, "Kron reduction of graphs with applications to electrical networks," *IEEE Trans. Circuits Syst. I, Reg. Papers*, vol. 60, no. 1, pp. 150–163, Jan. 2013.

[24] K. Walton and J. E. Marshall, "Direct method for tds stability analysis," *IEE Proc. D Control Theory Appl.*, vol. 134, no. 2, pp. 101–107, 1987.

[25] G. Lou, W. Gu, Y. Xu, W. Jin, and X. Du, "Stability robustness for secondary voltage control in autonomous microgrids with consideration of communication delays," *IEEE Trans. Power Syst.*, vol. 33, no. 4, pp. 4164–4178, Jul. 2018.

[26] R. Olfati-Saber, J. A. Fax, and R. M. Murray, "Consensus and cooperation in networked multi-agent systems," *Proc. IEEE*, vol. 95, no. 1, pp. 215–233, Jan. 2007.

Yuhua Du (Member, IEEE) received the B.S. degree in electrical engineering from Xi'an Jiaotong University, China, in 2013, and the Ph.D. degree in electrical and computer engineering from North Carolina State University, USA, in 2019. He was a Research Aide with Argonne National Laboratory in 2018. He is currently a Postdoctoral Fellow of Temple University. His research interests include voltage source converter modeling and control, microgrid distributed secondary control, and microgrid hardware-in-the-loop testbed.

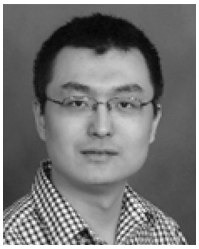

Xiaonan Lu (Member, IEEE) received the B.E. and Ph.D. degrees in electrical engineering from Tsinghua University, Beijing, China, in 2008 and 2013, respectively. From September 2010 to August 2011, he was a guest Ph.D. student with the Department of Energy Technology, Aalborg University, Denmark. From October 2013 to December 2014, he was a Postdoctoral Research Associate with the Department of Electrical Engineering and Computer Science, University of Tennessee, Knoxville. From January 2015 to July 2018, he was with Argonne National Laboratory, first as a Postdoctoral Appointee and then as an Energy Systems Scientist. In July 2018, he joined the College of Engineering, Temple University as an Assistant Professor. His research interests include modeling and control of power electronic inverters, hybrid AC and DC microgrids, and real-time hardware-in-the-loop simulation. He is a recipient of the 2020 Young Engineer of the Year Award in the IEEE Philadelphia Section. He is an Associate Editor of IEEE TRANSACTIONS ON INDUSTRIAL ELECTRONICS and IEEE TRANSACTIONS ON INDUSTRY APPLICATIONS, and an Editor of IEEE TRANSACTIONS ON SMART GRID. He serves as the Chair of the Industrial Power Converters Committee in the IEEE Industry Applications Society.

Wenyuan Tang (Member, IEEE) received the B.Eng. degree in electrical engineering from Tsinghua University, Beijing, China, in 2008, and the M.S. degree in electrical engineering, the M.A. degree in applied mathematics, and the Ph.D. degree in electrical engineering from the University of Southern California, Los Angeles, CA, USA, in 2010, 2014, and 2015, respectively. He was a Postdoctoral Scholar with the University of California at Berkeley, Berkeley, and Stanford University. He is currently an Assistant Professor with the Department of Electrical and Computer Engineering, North Carolina State University, Raleigh, NC, USA. His research interests include electricity markets, energy data analytics and machine learning, and control and optimization for power systems.